JCI insight

RESEARCH ARTICLE

T-bet+ B cells are induced by human viral infections and dominate the HIV gp140 response

James J. Knox,[1] Marcus Buggert,[1,2] Lela Kardava,[3] Kelly E. Seaton,[4] Michael A. Eller,[5,6] David H. Canaday,[7] Merlin L. Robb,[5,6] Mario A. Ostrowski,[8] Steven G. Deeks,[9] Mark K. Slifka,[10] Georgia D. Tomaras,[4] Susan Moir,[3] M. Anthony Moody,[11] and Michael R. Betts[1]

[1]Department of Microbiology, Perelman School of Medicine, University of Pennsylvania, Philadelphia, Pennsylvania, USA. [2]Center for Infectious Medicine, Department of Medicine, Karolinska Institutet, Karolinska University Hospital Huddinge, Stockholm, Sweden. [3]Laboratory of Immunoregulation, National Institute of Allergy and Infectious Diseases, NIH, Bethesda, Maryland, USA. [4]Duke Human Vaccine Institute; and Department of Surgery, Duke University Medical Center, Durham, North Carolina, USA. [5]US Military HIV Research Program, Walter Reed Army Institute of Research, Silver Spring, Maryland, USA. [6]Henry M. Jackson Foundation for the Advancement of Military Medicine, Bethesda, Maryland, USA. [7]Division of Infectious Disease, Case Western Reserve University School of Medicine, and Cleveland VA, Cleveland, Ohio, USA. [8]Departments of Immunology and Medicine, University of Toronto, Toronto, Ontario, Canada; Keenan Research Centre for Biomedical Science of St. Michael's Hospital, Toronto, Ontario, Canada. [9]Department of Medicine, University of California, San Francisco, San Francisco, California, USA. [10]Division of Neuroscience, Oregon National Primate Research Center, Oregon Health and Science University, Beaverton, Oregon, USA. [11]Duke Human Vaccine Institute; Department of Pediatrics; and Department of Immunology, Duke University Medical Center, Durham, North Carolina, USA.

Humoral immunity is critical for viral control, but the identity and mechanisms regulating human antiviral B cells are unclear. Here, we characterized human B cells expressing T-bet and analyzed their dynamics during viral infections. T-bet+ B cells demonstrated an activated phenotype, a distinct transcriptional profile, and were enriched for expression of the antiviral immunoglobulin isotypes IgG1 and IgG3. T-bet+ B cells expanded following yellow fever virus and vaccinia virus vaccinations and also during early acute HIV infection. Viremic HIV-infected individuals maintained a large T-bet+ B cell population during chronic infection that was associated with increased serum and cell-associated IgG1 and IgG3 expression. The HIV gp140–specific B cell response was dominated by T-bet–expressing memory B cells, and we observed a concomitant biasing of gp140-specific serum immunoglobulin to the IgG1 isotype. These findings suggest that T-bet induction promotes antiviral immunoglobulin isotype switching and development of a distinct T-bet+ B cell subset that is maintained by viremia and coordinates the HIV Env–specific humoral response.

Introduction

The HIV pandemic persists as one of the most significant global health problems (1). While antiretroviral therapy has greatly improved mortality rates, a preventive vaccine remains necessary to curtail the spread of HIV (2). Efforts have shifted to rationally based vaccine design, requiring an in-depth analysis of immune responses to identify and stimulate protective immunological correlates (3). Recent isolation and characterization of many naturally occurring HIV-specific broadly neutralizing antibodies demonstrates the capacity of humans to generate a potentially protective humoral response (4), but the B cells and mechanisms regulating humoral immunity to HIV remain poorly characterized. An improved understanding of the B cell response will identify interventional targets and inform rational vaccine design for HIV and other viruses for which broadly effective vaccines do not exist.

The humoral immune system is critical for control of multiple viruses during both acute and chronic phases of infection (5, 6), and most effective vaccines are thought to function by eliciting a protective humoral response (7). Humoral immunity is coordinated by memory B cells, antigen-specific subsets that can regulate the developing immune response via functions such as antigen presentation, cytokine

Conflict of interest: The authors have declared that no conflict of interest exists.

Submitted: January 19, 2017
Accepted: March 2, 2017
Published: April 20, 2017

Reference information:
JCI Insight. 2017;2(8):e92943. https://doi.org/10.1172/jci.insight.92943.

production, or differentiation into antibody-secreting cells (8–10). Memory B cells can also express different antibody isotypes that fulfill diverse spatiotemporal and pathogen-specific roles upon secretion (11, 12). Heterogeneity has been demonstrated within the origins, development, and functional capacity of human memory B cell populations differentiated by a variety of cell surface markers (12). Recent studies have begun to assess the contributions of B cell subsets during active immune responses using antigen-specific probes (13, 14), but the identity and regulation of virus-specific memory B cells during HIV and other viral infections remain poorly understood.

Transcription factors are critical regulators of memory B cell identity and function that can translate pathogen-specific cues into induction of appropriate humoral responses (15–18). Recent studies identified the immune cell–specific transcription factor T-bet as a critical regulator of murine antiviral B cell responses (6, 19). T-bet was originally described as controlling $CD4^+$ Th1 cell development and functionality (20), but T-bet also plays a role in B cell differentiation (21, 22). In mice, T-bet expression is required for isotype switching, functionality, and survival of $IgG2a/c^+$ memory B cells (18, 22, 23) and can also regulate the expression of the antiviral cytokine IFN-γ and the inflammatory homing receptor CXCR3 in this population (24, 25). Several groups recently examined the direct role of $T\text{-}bet^+$ B cells during murine viral infections; gamma herpes virus 68 induces an expansion of $T\text{-}bet^+$ B cells, the absence of which leads to infection exacerbation (19). Similarly, chronic lymphochoriomeningitis (LCMV) viremia is controlled to low levels only in the presence of $T\text{-}bet^+$ B cells via a chiefly IgG2a-dependent mechanism (6). We previously identified a subset of T-bet–expressing B cells in healthy human blood (26), and B cells expressing either *TBX21* transcript or T-bet protein have been described in the context of autoimmune disease, chronic hepatitis C infection, and malaria infection (27–31), but the biological niche of this population in humans has not been defined.

HIV infection is characterized by excessive viral replication and inflammation that induce a strong virus-specific humoral response and promote polyclonal B cell stimulation (32, 33). This B cell hyperactivation likely contributes to previously described B cell subset alterations in chronically infected individuals (33). The memory B cell compartment is particularly impacted by HIV, with decreased resting memory B cell numbers and an expansion of activated and atypical memory B cells that lack expression of the complement receptor CD21 (34, 35). We previously demonstrated that HIV-specific responses are overrepresented in $CD21^-$ memory B cells in viremic individuals (13), but the mechanisms regulating the B cell response to HIV are unclear.

In this study, we characterize $T\text{-}bet^+$ B cells in human peripheral blood and examine their role during HIV and other human viral infections. We identified $T\text{-}bet^+$ B cells as a distinct antigen-experienced population that demonstrates an activated, potentially antiviral phenotype and expands in response to acute viral infections. $T\text{-}bet^+$ B cells are maintained at a high frequency during chronic HIV infection and correlate with increased expression and secretion of IgG1 and IgG3, two human antibody isotypes critical for antiviral responses. This $T\text{-}bet^+$ population maintains the anti-gp140 B cell response and, via the expression of T-bet, likely biases gp140-specific antibodies to the IgG1 isotype. Our data identify $T\text{-}bet^+$ B cells as responders during both acute and chronic human viral infections and suggest this population orchestrates the humoral immune response to HIV.

Results

Defining subsets of human B cells that express T-bet. In order to define $T\text{-}bet^+$ B cell populations in human blood, we developed a panel to assess all major B cell subsets through expression of CD10, CD38, CD27, CD21, and IgD (subset gating and definitions in Supplemental Figure 1A; supplemental material available online with this article; https://doi.org/10.1172/jci.insight.92943DS1). In agreement with our previous study (26), significantly more memory B cells expressed T-bet compared with transitional and naive B cells (Figure 1, A and B), and plasmablasts (as determined by flow cytometry and RNA transcript analysis; data not shown). As T-bet is known to regulate Ig class switching to IgG2a/c in mice (22, 23), we further assessed the relationship between T-bet and human memory B cell surface Ig isotypes (Supplemental Figure 1B). T-bet was expressed at the highest frequency by IgG^+ cells, specifically those expressing IgG1 or IgG3, which are critical for antiviral responses (11) (Figure 1C). However, T-bet expression could also be detected to a lesser degree in subsets of B cells expressing the other tested Ig isotypes (Figure 1C).

To further define the characteristics of $T\text{-}bet^+$ memory B cells, we used CD21 and CD27 to delineate several previously described populations (35) (Figure 1D). The two $CD21^-$ subsets, activated memory (AM,

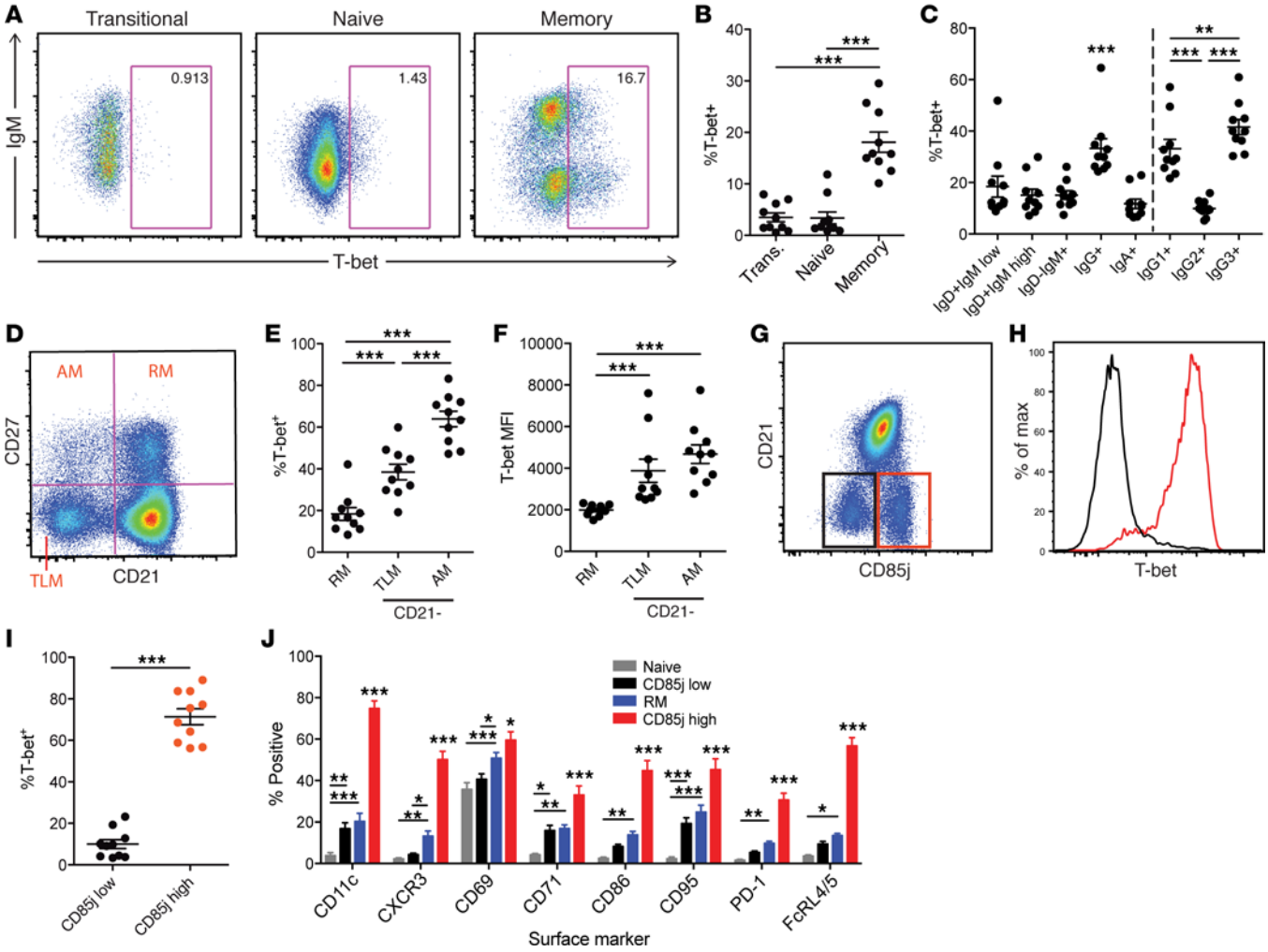

Figure 1. T-bet expression in memory B cell subsets from healthy human peripheral blood. (**A**) Representative flow cytometry plots of T-bet expression in peripheral blood B cell subsets from a single donor. (**B**) T-bet expression frequency per subset in a 10-donor cohort. Bars on this and all following plots represent mean ± SEM. Trans., transitional B cell.(**C**) T-bet expression frequency of memory B cells expressing different Ig isotypes. (**D**) CD21/CD27–based gating scheme of total CD38^{lo}CD10^{-} B cells from a representative donor. AM, activating memory, CD27^{+}CD21^{-}; RM, resting memory, CD27^{+}CD21^{+}; TLM, tissue-like memory, CD27^{-}CD21^{-}. (**E**) T-bet expression frequency of CD21/CD27–derived B cell subsets. (**F**) T-bet median fluorescence intensity (MFI) of T-bet^{+} cells from each B cell subset. (**G**) Gating of CD21^{-}CD85j^{hi} and CD21^{-}CD85j^{lo} B cell subsets from a representative donor's total CD38^{lo}CD10^{-} B cells. (**H**) T-bet expression histogram of CD85j-gated B cell subsets from donor depicted in **G**. (**I**) T-bet expression frequency of CD85j-gated B cell subsets in 10-donor cohort. (**J**) Expression frequency of homing receptors (CD11c, CXCR3), activation markers (CD69, CD71, CD86, CD95), and inhibitory receptors (PD-1, FcRL4/5) by CD38^{lo}CD10^{-} B cell subsets. Statistical comparisons in **B**, **C**, **E**, **F**, and **J** calculated using repeated-measures 1-way ANOVA with Tukey's multiple comparisons test. Statistical comparison in **I** calculated using paired *t* test. $^{*}P \geq 0.01$ to < 0.05; $^{**}P \geq 0.001$ to < 0.01; $^{***}P < 0.001$.

CD21^{-}CD27^{+}) and tissue-like memory (TLM, CD21^{-}CD27^{-}) B cells, expressed T-bet at the highest frequencies (Figure 1E) and at significantly higher levels per cell (Figure 1F) compared with resting memory (RM) cells, indicating a prominent role for T-bet in regulation of the peripheral CD21^{-} memory B cell compartment. Interestingly, we identified a bimodal expression pattern of T-bet in AM and TLM subsets (Supplemental Figure 1C). We therefore explored additional cell surface receptors to better demarcate CD21^{-}T-bet^{+} cells and found that this subset also highly expresses the inhibitory receptor CD85j (Figure 1, G–I). The CD21^{-}T-bet^{hi}CD85j^{hi} population (hereafter referred to as T-bet^{hi}CD85j^{hi} cells) was comprised of approximately half the TLM population and nearly all of the AM population, whereas the remaining TLM cells represent the CD21^{-}CD85j^{lo} population (Supplemental Figure 1, D and E). T-bet^{hi}CD85j^{hi} cells also highly expressed several homing receptors, activation markers, additional inhibitory receptors (Figure 1J), and demonstrated a diverse repertoire of Ig isotypes (Supplemental Figure 1F). Interestingly, T-bet^{hi}CD85j^{hi} cells highly expressed the transcription factor irrespective of surface Ig isotype expression (Supplemental Figure 1G), suggesting additional Ig isotype–independent roles for T-bet in this population. In summary,

Table 1. Yellow fever virus and vaccinia virus vaccine recipients

Vaccinia	Donor ID	Week 0	Week 1	Week 2	Week 3	Week 4	Week 25+
	12	Pre	7	14	21	28	180
	13	Pre	7	17	21	28	184
	501	Pre	7	15	22	29	183
	502	Pre	7	14	23	28	183
	503	Pre	7	14	21	28	181
	507	Pre	7	14	21	29	195
	548	Pre	7	14	21	28	271
Yellow Fever	**Donor ID**	**Week 0**	**Week 1**	**Week 2**	**Week 3**	**Week 4**	**Week 8+**
	4	Pre	8	15	20	28	184
	12	Pre	n/a	14	22	30	203
	558	1	n/a	15	22	29	218
	559	1	8	15	22	32	120
	565	1	9	16	23	30	60

Blood sample timing for $n = 7$ vaccinia virus vaccine recipients and $n = 5$ yellow fever vaccine recipients are depicted. Each row represents 1 donor with longitudinal samples collected at each day after vaccination. Columns show binning of sampling into weeks after vaccination.

we identified 2 populations of T-bet$^+$ B cells: an RM subset expressing T-bet at low levels and a subset distinguished by a lack of CD21 expression and high levels of CD85j that represents the main T-bet^{hi} B cell population in the peripheral blood of healthy human donors.

T-bet$^+$ B cells are induced during acute viral infections. T-bet$^+$ B cells have previously been shown to expand during acute LCMV and ghv68 infections in mice (6, 19); we therefore asked whether human T-bet$^+$ B cells might similarly be induced during human acute viral infections. To assess this, we examined B cell responses in human subjects vaccinated with yellow fever virus (YFV) and vaccinia virus (VV). These replicating live virus vaccines are thought to elicit durable protection via antibody-mediated mechanisms (7, 36–38), suggesting a critical role for B cells in this process. We analyzed T-bet expression within total memory B cells collected from the peripheral blood of vaccinated individuals on the day of vaccination, at weekly acute time points, and at a final time point ranging from 2 to 8 months after vaccination (Table 1). We identified the emergence of a T-bet$^+$ population as early as 2 weeks after YFV and VV vaccinations, which expanded and remained detectable in peripheral blood through postvaccination week 4 (Figure 2, A and B). The frequency of total T-bet$^+$ B cells peaked around week 4 in the majority of individuals receiving either YFV (Figure 2C) or VV (Supplemental Figure 2A) vaccination, suggesting that both vaccines stimulated a T-bet$^+$ B cell response. The T-bet^{hi}CD85j^{hi} B cell frequency also peaked at week 4 in YFV-vaccinated individuals (Figure 2D), and expansion was preceded by expression of the activation marker Ki67 in this population at postvaccination week 2 (Figure 2E). While T-bet^{hi}CD85j^{hi} cell expansion was not detected in all donors during VV vaccination (Supplemental Figure 2B), T-bet median fluorescence intensity (MFI) in T-bet^{hi}CD85j^{hi} cells was dynamic and peaked between weeks 3 and 4 during both YFV and VV responses (Figure 2F and Supplemental Figure 2C). These responses were not limited to a single surface Ig isotype, as T-bet expression increased in both IgM$^+$ and class-switched T-bet^{hi}CD85j^{hi} cells (Supplemental Figure 2, D and E). RM B cells, which normally express low levels of T-bet (Figure 1E), displayed increased T-bet expression frequencies in several VV vaccine recipients (Supplemental Figure 2F) but only in 1 YFV vaccine recipient (Supplemental Figure 2G). This RM T-bet response involved only a small subset of cells, as RM population size did not increase (data not shown) and T-bet MFI in the total population remained static during both vaccinations (Figure 2F and Supplemental Figure 2C). Interestingly, T-bet levels in plasmablasts also increased following each vaccination (Supplemental Figure 2, H and I). Together, these findings indicate that human live viral vaccinations stimulate an acute T-bet$^+$ B cell response and that the T-bet^{hi}CD85j^{hi} population may function as an early responder during acute viral infections.

YFV and VV vaccinations represent relatively controlled, low-inflammation infections. We therefore investigated whether T-bet$^+$ B cells similarly expand during acute HIV infection. To assess this, we obtained longitudinal samples from high-risk HIV-seronegative individuals who subsequently became infected with HIV from the US Military HIV Research Program RV217 early-capture HIV cohort (39). We analyzed

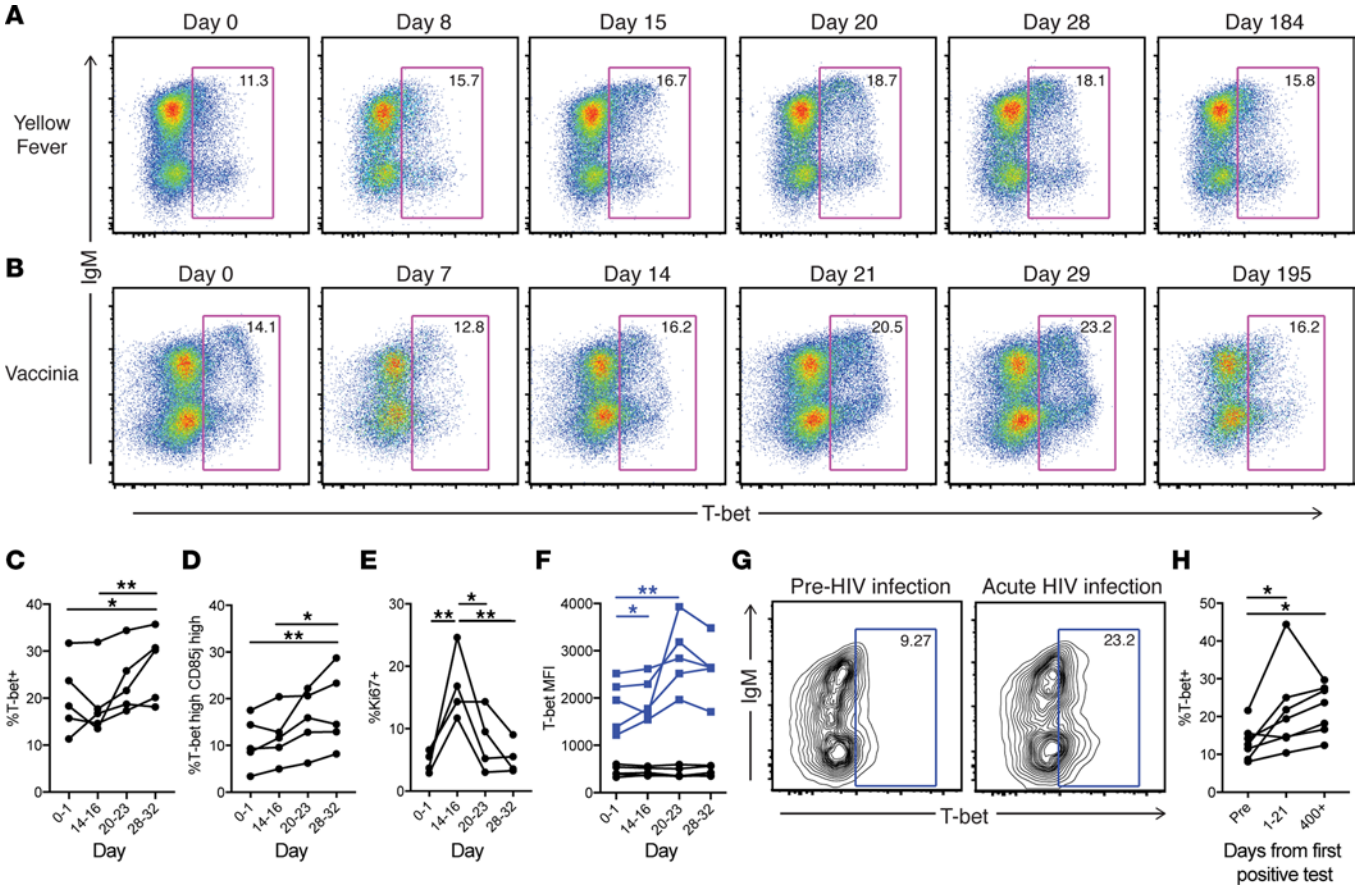

Figure 2. Longitudinal T-bet$^+$ B cell dynamics in yellow fever virus–vaccinated, vaccinia virus–vaccinated, or acutely HIV-infected individuals. Longitudinal T-bet expression in memory B cells of (**A**) a yellow fever vaccinee and (**B**) a vaccinia vaccinee. Time of blood sampling after vaccination is depicted. (**C**) T-bet expression frequency in memory B cells of yellow fever vaccinees (n = 5 for all plots except **E**). Donor samples were binned to organize approximate weekly time points. (**D**) T-bet^{hi}CD85j^{hi} cell frequency of total memory B cells in yellow fever vaccinees. (**E**) Ki67 expression frequency of T-bet^{hi}CD85j^{hi} cells in yellow fever vaccines (n = 4). (**F**) T-bet median fluorescence intensity (MFI) of T-bet^{hi}CD85j^{hi} cells (blue) and resting memory (RM) cells (black) in yellow fever vaccinees. No statistical differences were observed between RM time points. (**G**) T-bet expression in memory B cells of an acutely HIV-infected individual before infection and shortly after peak of viremia. (**H**) Memory B cell T-bet expression frequency from 7-donor cohort of acutely HIV-infected individuals at preinfection, acute, and chronic infection time points. Note that intracellular T-bet staining of early acute HIV samples in **G** and **H** was performed using a BD Cytofix/Cytoperm Kit. Statistical comparisons in **C**, **D**, **E**, **F**, and **H** calculated using repeated-measures 1-way ANOVA with Tukey's multiple comparisons test. *$P \geq 0.01$ to < 0.05; **$P \geq 0.001$ to < 0.01.

T-bet expression in total memory B cells (Supplemental Figure 1A) from preinfection, early acute, and early chronic infection time points (Table 2). During early acute infection (days 1–21 after first positive HIV RNA test), 6 out of 7 individuals demonstrated a rapid increase in the frequency of T-bet–expressing memory B cells, supporting the role of these cells as part of an early antiviral response (Figure 2, G and H). Similar to YFV and VV vaccinations, we also observed increased T-bet MFI in plasmablasts at this acute time point (Supplemental Figure 2J). These 6 individuals remained viremic into early chronic infection and concomitantly maintained elevated T-bet levels, suggesting a relationship between continued viral replication and maintenance of this expanded population (Figure 2H).

HIV infection maintains an expanded T-bet$^+$ B cell population. Having observed the rapid expansion and sustained expression of T-bet$^+$ B cells in acute to early chronic HIV infection, we next examined T-bet expression in memory B cells from chronically infected HIV$^+$ cohorts with different viral loads (VLs): viremic HIV progressors (progressors, VL > 10,000 copies/ml); viremic controllers (VCs, VL 41–1,800 copies/ml); elite controllers (ECs, VL < 40 copies/ml); aviremic individuals on antiretroviral therapy (ART, VL < 40 copies/ml); and HIV-negative controls (Supplemental Tables 1 and 2). We identified a significant expansion of T-bet$^+$ memory B cells in HIV-infected progressors and VCs compared with healthy controls (Figure 3, A and B). In progressors (individuals with the highest viremia) this expansion was comprised almost entirely of T-bet^{hi}CD85j^{hi} B cells (Figure 3C) and coincided with higher expression levels (MFI) of T-bet (Figure 3D).

Table 2. RV217 Early Capture HIV cohort

Donor ID	Day relative to first pos. test	VL (copies/ml)	CD4 count (cells/μl)
10,374	–194	n/a	n/a
	21	10,965	775
	407	17,783	446
30,507	–289	n/a	n/a
	17	1,122	1,574
	413	7,585	n/a
40,067	–467	n/a	n/a
	1	229,087	565
	403	23,988	425
40,134	–69	n/a	n/a
	2	2,454,709	435
	433	13,804	n/a
40,250	–173	n/a	n/a
	14	4,677,351	522
	420	16,596	461
40,283	–478	n/a	n/a
	1	398,107	376
	425	50,199	n/a
40,353	–41	n/a	n/a
	14	162,181	574
	415	3,388	448

Longitudinal samples were obtained at preinfection, acute, and chronic infection time points for $n = 7$ donors, with the collection date listed as day relative to first HIV-positive RNA test. Viral load (VL) and CD4 counts are listed where available. Individuals were therapy-naive at the time of sampling.

Absence of detectable viremia in ECs and ART individuals was associated with decreased T-bet$^+$ B cell population size in many donors compared with viremic individuals (Figure 3B), which could be explained in part by diminished T-bet^{hi}CD85j^{hi} expansion in these cohorts (Supplemental Figure 3A). We also observed a trend toward elevated T-bet expression frequencies in RM B cells in all HIV$^+$ cohorts (Supplemental Figure 3B); however, similar to our findings in HIV-negative donors (Figure 1F), RM cell T-bet expression levels (MFI) remained low (data not shown). Together, our findings indicate that chronic HIV viremia drives T-bet expression in memory B cells and maintains the expansion of the T-bet^{hi}CD85j^{hi} subset.

We further observed increased T-bet MFI in plasmablasts of viremic individuals (Supplemental Figure 3C), suggesting together with our acute infection findings that viral replication also promotes low-level T-bet expression in plasmablasts. As T-bet is associated with specific IgG isotypes (Figure 1C), we hypothesized that the maintenance of elevated T-bet expression in B cells and plasmablasts during HIV infection might alter memory B cell surface IgG isotype distribution and serum Ig repertoires in these individuals. We therefore analyzed memory B cells from HIV-negative individuals and progressors and found increased frequencies of IgG1- and IgG3-expressing memory B cells during HIV infection (Figure 3E). To explore possible downstream effects on secreted Ig, we next assessed the isotypes of total serum Ig from progressors and age/ethnicity–matched HIV-negative controls and found approximately 2-fold increases in titers of IgG1 and IgG3 in progressors as compared with controls (Figure 3F). IgG1 titers in viremic subjects positively correlated with the frequency of T-bet$^+$ memory B cells (though this did not reach statistical significance due to a single outlier), while IgG2, IgG3, IgG4, and IgA titers displayed no relationship (Figure 3G). IgM titers also positively correlated with T-bet expression frequency (Figure 3G), suggesting that activation events in early memory B cell differentiation may be skewed by T-bet expression. In summary, HIV drives the expansion and maintenance of T-bet$^+$ B cells that correlate with an overrepresentation of surface-expressed and soluble IgG1 and IgG3 during viremic infection.

T-bet^{hi}CD85j^{hi} B cells represent a transcriptionally distinct memory population. Seeking to better define the overall ramifications of T-bet expression on the B cell pool, we next investigated the transcriptional environment of T-bet$^+$ B cells, using CD85j^{hi} phenotype as a surrogate marker, and whether HIV infection alters T-bet$^+$ B cell transcriptional patterns using Fluidigm Biomark quantitative RNA analysis. Figure 4A depicts transcript expression levels of 91 selected target genes, including transcription factors, activation and inhibitory receptors, trafficking receptors, cell survival/death proteins, and other B cell–relevant genes within sorted B cell subsets from 4 HIV-negative donors. Unbiased clustering analysis of gene expression data demonstrated consistent clustering of B cell subsets between donors, indicating that our chosen panel clearly differentiates peripheral B cell populations (Figure 4A). T-bet^{hi}CD85j^{hi} cells' transcriptional signature included highest expression of the Ig class switching and somatic hypermutation enzyme *AICDA*, the glycosylation enzyme *B4GALT3*, transcription factors *IKZF1* (Ikaros) and *SOX5*, the inhibitory receptor *SIGLEC6*, and, importantly, *TBX21* (T-bet) (Figure 4A). CD85j^{hi} cells shared high expression of *CCR6*, *FCRL3*, *FCRL4*, *NFIL3*, *PBX4*, and *TNF* with RM cells, *FCRL5* and *TOX2* with plasmablasts, and *BATF*, *CASP3*, *CD27*, *FAS*, *FUCA2*, *FUT8*, and *POU2AF1* with both populations (Figure 4A).

To interrogate transcriptional similarity between T-bet^{hi}CD85j^{hi} cells and the other sorted B cell subsets in an unbiased way, we performed t-distributed stochastic neighbor embedding (tSNE) analysis of the transcript expression results (Figure 4B). T-bet^{hi}CD85j^{hi} cells were transcriptionally dissimilar to antigen-inexperienced B cells and clustered near to, but distinct from, RM B cells and plasmablasts,

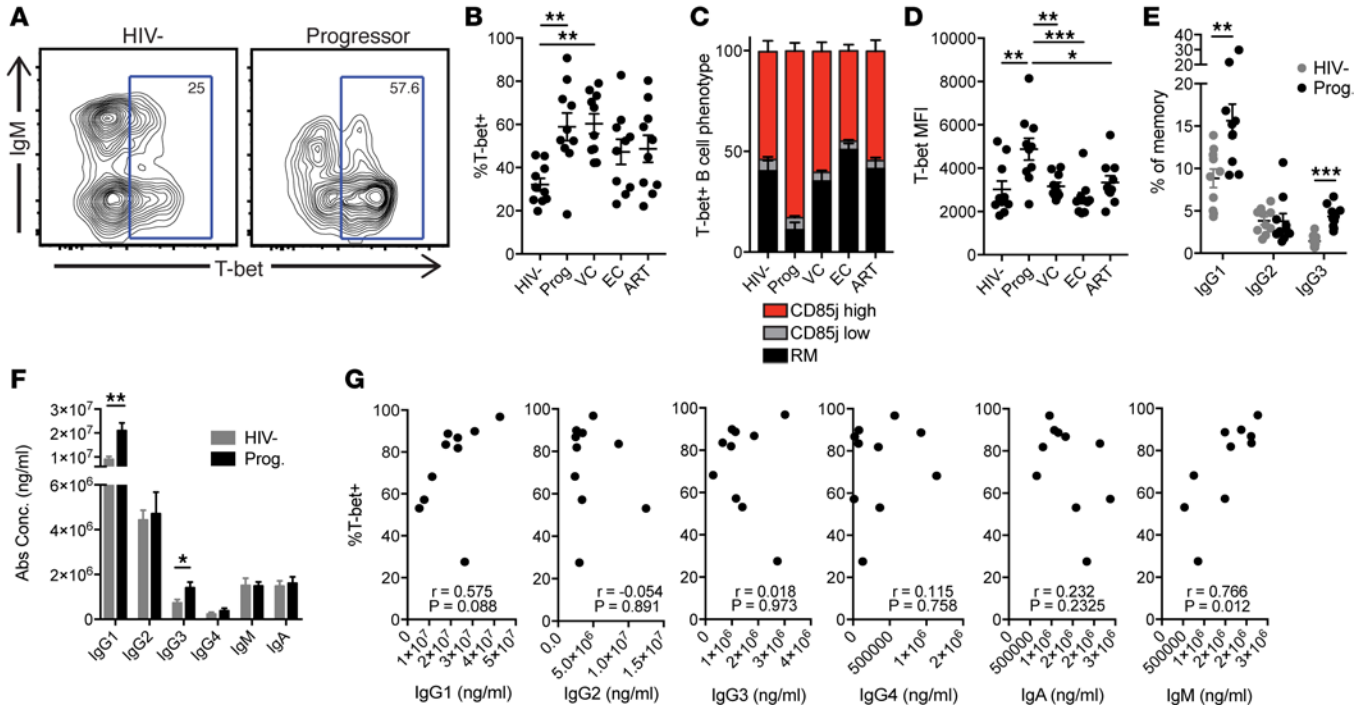

Figure 3. T-bet expression in B cells and antibody isotype repertoires during HIV infection. (**A**) T-bet expression in memory B cells of a representative HIV-negative donor and an HIV$^+$ chronic progressor (progressor). (**B**) T-bet expression frequency of memory B cells in HIV-negative, progressor, HIV$^+$ viremic controller (VC), HIV$^+$ elite controller (EC), and HIV$^+$ antiretroviral therapy–treated donors (ART); n = 10 donors per group. Statistical comparison calculated using 1-way ANOVA with Tukey's multiple comparisons test. (**C**) Phenotype of T-bet$^+$ B cell population from each cohort in **B**. Bars represent SEM. (**D**) T-bet median fluorescence intensity (MFI) of total T-bet$^+$ cells from each cohort. Statistical comparison calculated using 1-way ANOVA with Tukey's multiple comparisons test. (**E**) Frequency of IgG isotype–expressing B cells within total memory B cell compartment of HIV-negative individuals and progressors (HIV$^+$) (n = 10 donors per group). Horizontal bars in **B**, **D**, and **E** represent the mean ± SEM. Statistics in **E** and **F** calculated using unpaired t test. (**F**) Absolute concentration of total serum antibodies by isotype from progressor (HIV$^+$) and age/ethnicity–matched HIV-negative cohorts (n = 10 donors per group). (**G**) Correlations between T-bet expression frequency in memory B cells and serum antibody titers (ng/ml). Statistics calculated using Spearman correlation. *P ≥ 0.01 to < 0.05; **P ≥ 0.001 to < 0.01; ***P < 0.001.

further suggesting this is an antigen-experienced population. Interestingly, CD85j^{lo} B cells, the CD21$^-$T-bet$^-$ counterpart of our cells of interest, were more similar to the antigen-inexperienced subsets (naive, transitional; Figure 4B), suggesting these are relatively unrelated to T-bet^{hi}CD85j^{hi} cells and confirming the previously described population heterogeneity within the TLM phenotype (CD21$^-$CD27$^-$; ref. 40).

We next set out to establish a functional connection between T-bet and the transcriptional targets it might regulate in T-bet^{hi}CD85j^{hi} B cells. We focused on the B cell–specific enzyme activation–induced cytidine deaminase (AID, or *AICDA* as transcript), given its important role in antibody affinity maturation (41) and its elevated transcript expression in T-bet^{hi}CD85j^{hi} cells from both HIV-negative individuals and progressors (Supplemental Tables 1 and 3, and Figure 4C). To examine the potential regulation of *AICDA* transcript expression by T-bet, we performed siRNA-mediated downregulation of T-bet in primary CD21$^-$CD27$^-$ B cells from progressors with high T-bet expression frequencies in this subset (mean 93.6% T-bet$^+$, range 81.2% to 97.6%; Supplemental Figure 4A), as previously described (42); cells consistently retained their CD85j^{hi} phenotype following nucleofection (Supplemental Figure 4B). CD21$^-$CD27$^-$ B cells were chosen as a representation of the T-bet^{hi}CD85j^{hi} population because they can be identified and sorted via negative selection, avoiding potential ligation effects of CD85j-specific antibodies. T-bet siRNA knockdown reduced levels of *AICDA* by 44% compared with control siRNA, indicating that T-bet at least partially regulates expression of *AICDA* in this population (Figure 4D).

Finally, we asked whether chronic HIV infection might selectively induce transcriptional changes in T-bet^{hi}CD85j^{hi} cells and therefore potentially impact their functionality. We compared RNA transcript levels of our 91-member panel in T-bet^{hi}CD85j^{hi} cells between HIV-negative individuals (n = 4) and progressors (n = 5) and found that T-bet^{hi}CD85j^{hi} cells appear largely similar regardless of HIV infection status (Figure 4E). These findings suggest that, while viremic HIV infection greatly expands the

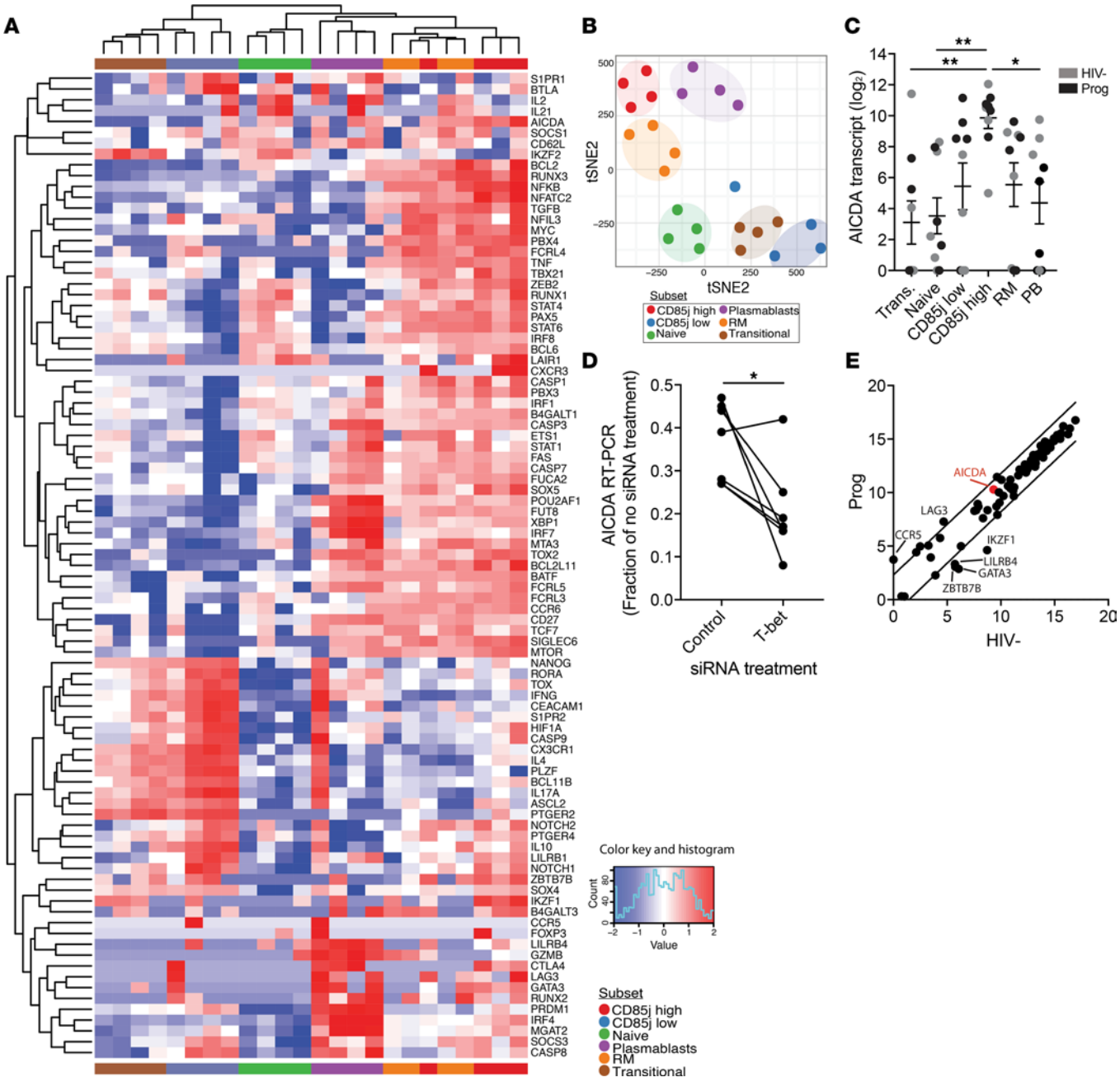

Figure 4. Transcriptional analyses of T-bet^{hi}CD85j^{hi} cells and other B cell subsets in HIV-negative donors and during HIV infection. (**A**) Heatmap depicting relative RNA transcript expression levels for 91 targets (1 per row) in HIV-negative donors (n = 4). Each column represents a specific B cell subset (colored bars above and below heatmap) sorted from 1 donor. (**B**) t-Distributed stochastic neighbor embedding (tSNE) analysis of transcriptional relationships between sorted B cell subsets from 4 healthy donors. Each color represents a sorted B cell subset and clusters are highlighted with the corresponding color. (**C**) *AICDA* transcript expression (log_2 units) of HIV-negative donors (gray; n = 4) and progressors (black; n = 5) per B cell subset. Trans., transitional; RM, resting memory; PB, plasmablast. Each data point represents transcript expression from 1 individual. Horizontal bars represent the mean ± SEM. Statistical comparison calculated using repeated-measures ANOVA with Tukey's multiple comparisons. (**D**) Quantitative reverse transcription PCR of *AICDA* transcript in CD21$^-$CD27$^-$ B cells of progressors transfected with control or T-bet siRNA. Values represent *AICDA* transcript level as a fraction of no-siRNA treatment condition. Statistical comparison calculated using paired t test. (**E**) Comparison of transcript expression levels for 91 gene targets between healthy donors (n = 4) and progressors (n = 5). Each data point represents the mean expression value calculated for HIV-negative donors (x value) and progressors (y value). Lines represent 90% prediction bands of calculated linear regression. Activation-induced cytidine deaminase (*AICDA*) transcript is depicted in red. *$P \geq 0.01$ to < 0.05; **$P \geq 0.001$ to < 0.01 (**C** and **D**).

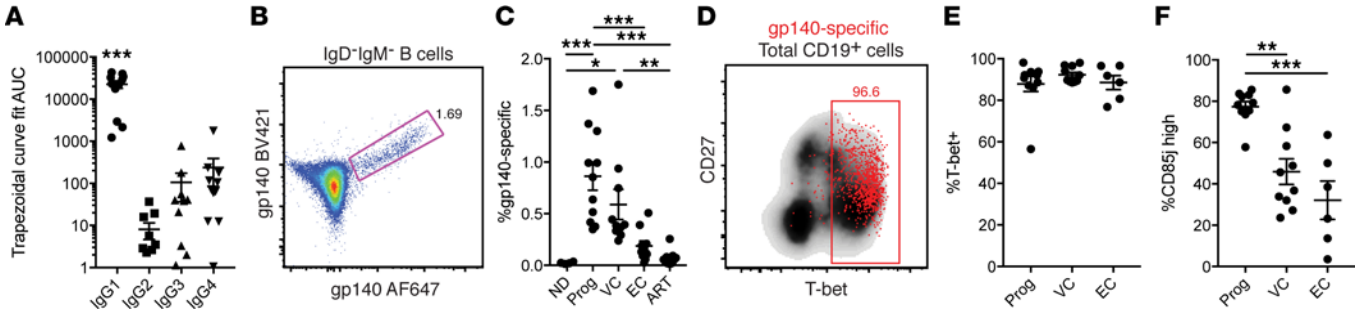

Figure 5. gp140-specific memory B cell phenotypes and serum Ig isotypes. (**A**) gp140-specific serum Ig titers by isotype from progressors (n = 10). Titers were normalized using age/ethnicity–matched controls. Statistical comparison calculated using repeated-measures 1-way ANOVA with Tukey's multiple comparisons test. (**B**) Representative staining of gp140-specific class-switched (IgD^-IgM^-) memory B cells from a progressor. (**C**) Frequency of gp140-specific cells within total class-switched memory B cells by cohort. n = 10 for all cohorts except progressors (n = 11). (**D**) T-bet expression of gp140-specific B cells (red) and total B cells (black) from a representative progressor. (**E**) Frequency of T-bet expression within gp140-specific cells from HIV^+ cohorts (n = 10 progressors, n = 10 viremic controllers [VC], n = 6 elite controllers [EC]). All donors with less than 40 gp140-specific cells (including all antiretroviral therapy [ART] individuals) were excluded from analyses in **E** and **F**. No statistical differences were observed between donor groups. (**F**) Frequency of gp140-specific cells with T-$bet^{hi}CD85j^{hi}$ phenotype by cohort. For **C**, **E**, and **F**, statistical comparisons were calculated using 1-way ANOVA with Tukey's multiple comparisons test. *$P \geq 0.01$ to < 0.05; **$P \geq 0.001$ to < 0.01; ***$P < 0.001$.

T-$bet^{hi}CD85j^{hi}$ population, it does not overtly alter the transcriptional environment of these cells during the course of infection.

HIV infection primarily drives a T-bet^+ B cell response to HIV envelope protein gp140. Finally, we examined the relationship between T-bet^+ B cells and the B cell response to HIV, focusing on the Env-specific response since this antigen is the relevant antibody target during HIV infection (32). Using a group M consensus sequence–derived gp140 protein to capture soluble Ig in an ELISA format, we analyzed the isotype repertoire of the gp140-specific Ig in serum of progressors (Supplemental Table 1) and found that, in agreement with previous studies (43–48), Env-specific responses are dominated by IgG1 isotype antibodies (Figure 5A), the most frequent IgG isotype associated with T-bet–expressing B cells. To directly connect this expanded Env-specific IgG1 usage to the cellular component of the response, we used gp140 protein fluorophore probes to identify gp140-specific B cells via flow cytometry, as previously described (49) (Figure 5B). Progressors, several of which were estimated to be in the early acute phase of infection, at less than 3 months HIV^+ (see Supplemental Table 3), demonstrated a mean gp140-specific B cell frequency of 0.86% of class-switched B cells in peripheral blood, and this frequency was diminished in HIV^+ cohorts with lower viremia (Figure 5C). Interestingly, nearly all gp140-specific B cells expressed T-bet, regardless of the HIV^+ donor's VL (Supplemental Tables 2 and 3; Figure 5, D and E). gp140-specific B cells from HIV viremic individuals consistently demonstrated a T-$bet^{hi}CD85j^{hi}$ phenotype, while the gp140-specific B cell response in subjects with lower or controlled viremia was composed of both T-$bet^{hi}CD85j^{hi}$ cells and RM B cells (Figure 5F and data not shown). Taken together, these findings demonstrate that the humoral immune response to HIV Env is specifically coordinated by the T-bet^+ memory B cell population and suggests induction of this transcription factor as a mechanism driving the predominantly IgG1-based Ig response to the virus.

Discussion

The identity of the cells orchestrating the humoral response to human viruses such as HIV has remained unclear. To address this issue, we assessed the phenotype and dynamics of B cells expressing T-bet, a known regulator of Th1-type immunity across cell lineages, during human viral infections. We identified T-bet^+ B cells as a distinct, activated subset enriched for antiviral Ig isotypes and expressing a specific trafficking receptor profile. The T-bet^+ B cell population, normally a small fraction of total B cells, transiently expands in response to acute YFV, VV, and HIV infection. However, during chronic HIV infection, viremia maintains elevated T-bet^+ B cell frequencies that are associated with increased serum IgG1 and IgG3 titers. These T-bet^+ cells dominate the HIV Env-specific B cell response and likely skew the anti-Env serum Ig repertoire to the IgG1 isotype.

T-bet is considered to function as a master regulator of Th1-type immunity (50), and T-bet is known to promote antiviral B cell responses by driving IgG2a/c class switching in mice (6, 19, 22, 23). Our findings suggest that T-bet similarly regulates human B cells during Th1 immune responses, as we clearly demonstrate

viral infection–induced T-bet expression in human B cells. Our results also identify Ig isotype diversification as a key effect of this T-bet induction; we described an association between T-bet and the IgG1 and IgG3 isotypes in healthy individuals and, importantly, observed increased frequencies of IgG1$^+$ and IgG3$^+$ memory B cells in viremic HIV$^+$ donors that maintain elevated T-bet expression. Memory B cells do not actively secrete Ig; however, viremic HIV$^+$ individuals also displayed increased T-bet MFI in plasmablasts, increased total IgG1 and IgG3 serum titers, and an IgG1-dominated Env-specific serum Ig response, suggesting IgG1$^+$ and IgG3$^+$ antibody-secreting cells readily differentiate from or share a similar origin with IgG1$^+$ and IgG3$^+$ memory B cells. It is unclear why IgG3 antibodies are not more prevalent within the anti-Env Ig repertoire during chronic HIV infection when T-bet expression is high, but IgG3 levels have been demonstrated to peak early during HIV infection and wane over time (32). It is possible that sustained HIV viremia drives recurrent germinal center reentry and isotype switching of memory B cells, which could promote splicing out of the proximally located γ3 gene from the constant region locus as the infection progresses; indeed, a recent study suggests class-switching of IgG3$^+$ B cells would likely give rise to either IgG1$^+$ or IgG2$^+$ cells (51). Together, our findings suggest T-bet expression in B cells coordinates the IgG1-dominated anti-Env response and likely regulates antibody isotype selection during other human viral infections.

Despite the relationship between T-bet and IgG isotypes, we also observed activation of the T-bet$^+$IgM$^+$ population in response to acute YFV and VV infections. While further experiments are necessary to determine if these IgM$^+$ memory cells are particularly prone to IgG1 or IgG3 isotype switching, these observations suggest additional Ig isotype-independent roles for T-bet in human B cells. T-bet may influence additional Ig properties, as T-bet^{hi}CD85j^{hi} cells demonstrate elevated RNA transcript levels of *B4GALT3*, a galactosyltransferase that may alter antibody glycosylation (52), and *AICDA*, the enzyme critical for somatic hypermutation that leads to improved antibody affinity (41). While AID expression is tightly controlled by multiple factors (53), our findings suggest that T-bet partially regulates *AICDA* transcript expression, although it is unclear whether this occurs by direct or indirect mechanisms. In doing so, T-bet may promote Ig mutation, and a recent murine study supports this notion by demonstrating relatively high mutation rates in Ig from T-bet–expressing B cells (54). However, Ig mutation may be impaired in subsets of T-bet$^+$ B cells during progressive HIV infection, as we recently demonstrated diminished mutation levels in HIV-specific Ig derived from TLM cells as compared with RM cell–derived Ig (55). Future studies should examine whether relatively low TLM Ig mutation rates are typical (i.e., observed in healthy individuals mounting successful humoral responses) or are instead reflective of immunopathology specific to chronic HIV infection; in support of the latter possibility, malaria-specific Ig derived from TLM-phenotype B cells displayed higher mutation rates than those derived from RM cell counterparts (56). Lastly, T-bet expression also influences Ig-independent functions and properties; similar to mice (19, 25), T-bet likely regulates the expression of homing receptors CXCR3 and CD11c in human B cells, potentially granting specific tissue- and inflammation-homing properties to T-bet$^+$ cells. Murine studies further suggest T-bet$^+$ B cells in the spleen efficiently present antigen (57) and can be stimulated to produce the cytokine IFN-γ (24).

Our study identified a heterogeneous T-bet–expressing B cell population in human blood comprised of 2 main subsets: T-bet^{hi}CD85j^{hi} cells (CD21$^-$T-bet^{hi}CD85j^{hi}) and T-bet–expressing RM cells (CD21$^+$CD27$^+$T-bet^{lo}). T-bet^{hi}CD85j^{hi} cells expand in response to acute human viral infections (YFV and VV vaccinations) and closely resemble age-associated B cells, a T-bet$^+$ population in mice that accumulates with age, produces pathogenic autoantibodies, and is critical for murine antiviral responses (6, 19, 58, 59). We also observed involvement of T-bet$^+$ B cells in the response to HIV infection, as T-bet was rapidly induced in B cells during the acute phase and T-bet^{hi}CD85j^{hi} cells maintained the Env-specific B cell response during chronic viremic HIV infection, with a reduction in T-bet^{hi}CD85j^{hi} population size following natural or therapy-mediated control of viremia. Together, our findings suggest T-bet^{hi}CD85j^{hi} cells are a major component of acute and chronic antiviral B cell responses and, in the setting of HIV, are responsive at a population level to modulation of viremia and immune activation. In contrast to T-bet^{hi}CD85j^{hi} cells, we did not observe significant expansion or activation of T-bet$^+$ RM cells in most individuals following YFV and VV vaccination, and reduction of viremia during chronic HIV infection did not affect T-bet$^+$ RM cell population size. Our findings suggest T-bet$^+$ RM cells do not play an active role during acute antiviral B cell responses and do not depend on viral replication for maintenance. While the origin and functions of this population remain unclear, T-bet$^+$ RM cells may represent quiescent descendants of T-bet^{hi}CD85j^{hi} cells that maintain long-lived antiviral memory, as acutely activated virus-specific B cell clones have been shown to seed the RM population following resolution of acute infection (14).

We and others have previously demonstrated an expansion of CD21$^-$ B cell subsets induced by Th1-type human infections, including HIV, malaria, and hepatitis C (30, 31, 34, 35, 60–63), and expansion of a clonal CD21$^-$ subset has been described during hepatitis B– and hepatitis C–associated mixed cryoglobulinemia (64–66). Interestingly, maintenance of expanded CD21$^-$ cells in each of these infections appears to be dependent upon pathogen load (34, 35, 60, 67–69). Our current findings, combined with the similar CD21$^-$ B cell phenotypes described in these studies, suggest that CD21$^-$ B cell expansion associated with these various Th1-type infections may in part be explained by infection-induced T-bet expression and expansion of T-bet^{hi}CD85j^{hi} cells. In support of this hypothesis, murine experiments suggest the T-bet$^+$ B cell phenotype is induced by concerted actions of pathogen-derived nucleic acids (TLR7 or TLR9 stimulation; refs. 15, 19, 58, 59, 70, 71) and cytokines produced during Th1-type infections (IFN-γ and IL-21; refs. 22, 24, 71) on B cells. Still, additional studies are necessary to determine the relationship between acute viral infection–induced T-bet^{hi}CD85j^{hi} cells and these chronic infection–expanded CD21$^-$ B cell subsets. Interestingly, observational human studies further demonstrate similar CD21$^-$ B cell expansion during various autoimmune diseases (27–29, 72, 73), and murine models indicate TLR sensing can stimulate T-bet expression to drive expansion of autoantibody-producing B cells (22, 58), suggesting CD21$^-$T-bet$^+$ B cells may also play a role in human autoimmune diseases.

While our acute infection observations suggested T-bet$^+$ B cells generally represent a component of the antiviral B cell response, we specifically demonstrated that T-bet$^+$ B cells comprise nearly the entire detectable peripheral B cell HIV Env memory response, beginning at least during early (<3 months HIV$^+$) infection. As such, most gp140-specific antibodies likely derive from descendants of the T-bet$^+$ B cell population or share a similar T-bet–regulated origin in both progressors and individuals controlling viremia. This likely also includes HIV-specific broadly neutralizing antibodies, but requires further assessment as previous studies that isolated broadly neutralizing antibodies from B cells generally did not consider the nature of the cells. An important question remaining is the degree to which T-bet$^+$ B cells and derived antibodies contribute to control of viremia during HIV and other viral infections. Indeed, while a murine study demonstrated the requirement of T-bet$^+$ B cells to control chronic LCMV viremia to low levels (6), the role of B cells and Ig in ongoing control of HIV/SIV remains controversial (74–78). However, it is highly likely that an efficacious HIV vaccine will need to induce HIV Env–specific broadly neutralizing antibodies. As such, our results directly demonstrate the importance of T-bet–expressing B cells to the HIV-specific humoral response.

Methods

Study participants. Acute infection studies: 5 healthy, HIV-negative individuals received live-attenuated YFV-17D vaccine (YF-Vax, Sanofi Pasteur) and 7 different healthy, HIV-negative individuals received live vaccinia smallpox vaccine (Dryvax, Wyeth Laboratories). Peripheral blood mononuclear cell (PBMC) samples were obtained on or near day of vaccination and at several subsequent time points (see Table 1 for donor information). Seven acutely infected HIV$^+$ donors were enrolled in the RV217 Early Capture HIV Cohort run by the US Military HIV Research Program. PBMC sample timing was calculated relative to first positive HIV RNA test (Abbot Real-Time HIV-1 assay, Abbot Laboratories). Samples included a pre-infection time point (ranging 478–41 days previous to first positive HIV RNA test), an early acute infection time point (ranging 1–21 days after first positive test; these were collected during or shortly after peak acute viremia and are considered to represent an early acute infection time point), and a chronic infection time point (see Table 2). Individuals were antiretroviral therapy-naive at all sample time points assessed.

Chronic HIV infection studies: PBMCs and serum from ART-naive, viremic HIV$^+$ individuals (referred to as progressors) and PBMCs from ART-treated, aviremic HIV$^+$ individuals (referred to as ART) were obtained from the University of Pennsylvania Center for AIDS Research (CFAR; see Supplemental Tables 1 and 3). HIV-negative serum samples age- and ethnicity-matched to the ART-naive, viremic HIV$^+$ individuals were obtained from Case Western University. PBMCs from VCs and ECs were obtained from individuals enrolled in the SCOPE study at the University of California San Francisco (see Supplemental Table 2). Additional progressor PBMCs were obtained from the University of Toronto (see Supplemental Table 3). Healthy HIV-negative human donor PBMC samples were obtained from the University of Pennsylvania Human Immunology Core.

Antibody reagents. The following antibodies were obtained from Biolegend: CD19 BV785 (clone HIB19), CD3 APC-Cy7 (clone UCHT1), IgM BV605 (clone MHM-88), CD21 PECy7 (clone Bu32), CD27 BV650 (clone O323), CD38 BV421 (clone HIT2), CXCR3 BV711 and APC (clone G025H7),

CD86 BV605 (clone IT2.2), CD10 BV605 (clone HI10a), CD71 FITC (clone CY1G4), and PD-1 BV421 (clone EH12.2H7). The following antibodies were obtained from BD Biosciences: CD14 APC-Cy7 (clone MØP9), CD16 APC-Cy7 (clone 3G8), IgD PECF594 and AF700 (clone IA6-2), IgG AF700 (clone G18-145), CD85j FITC (clone GHI/75), Ki67 AF700 and FITC (clone 56), CD21 BV421 (B-ly4), and CD95 PECy5 (clone DX2). The following antibodies were obtained from eBiosciences: T-bet PE and PECy7 (clone eBio4B10), CD10 PECy5 (clone eBioCB-CALLA), CD11c PECy5.5 (clone 3.9), and CD85j APC (clone HP-F1). CD69 PECy5 (clone TP1.55.3) was obtained from Beckman Coulter. The following antibodies were obtained from Southern Biotech: IgG1 PE (clone HP6001), IgG2 AF488 (clone HP6002), and IgG3 AF647 (clone HP6050). IgA FITC (polyclonal) was obtained from Invitrogen. FcRL4/5 antibody (clone 2A6) was gifted by Max D. Cooper (Emory University, Atlanta, Georgia, USA); this antibody was initially characterized as FcRL4 specific, but a recent study demonstrated that clone 2A6 reacts with both FcRL4 and FcRL5 (56).

Antibody staining, flow cytometry acquisition, and analysis. Cryopreserved PBMCs were thawed, counted, examined for viability, and rested overnight at 37°C and 5% CO_2 in RPMI with 10% FBS, 2 mM L-glutamine, 100 U/ml penicillin, and 100 mg/ml streptomycin added. All incubations during the following staining process were performed at room temperature in the dark. On the following morning, PBMCs were washed with PBS and stained for viability with Aqua amine-reactive viability dye (Invitrogen) for 10 minutes. Cells were stained with a prepared cocktail of surface antibodies for 25 minutes, washed once with PBS plus 0.1% sodium azide and 1% BSA, and fixed/permeabilized using the eBiosciences FoxP3 Transcription Factor buffer kit (catalog 00-5523-00). Intracellular targets were stained with a separately prepared cocktail of antibodies for 60 minutes, washed with the eBioscience kit buffer, fixed with PBS plus 1% paraformaldehyde, and stored in the dark at 4°C until acquisition. RV217 cohort samples (Figure 2, G and H) were stained identically except a BD Cytofix/Cytoperm Kit (catalog 554722) was used to fix/permeabilize cells for intracellular staining. Compensation controls were produced with antibody capture beads (BD Biosciences) for each antibody and ArC Amine Reactive beads (Thermo Fischer Scientific) for Aqua amine-reactive dye. All flow cytometry data were collected on a modified LSR II (BD Immunocytometry Systems). Data were analyzed using FlowJo software (Tree Star). Graphs were created and statistical analysis was performed using GraphPad Prism (version 7.0a).

HIV gp140 probe staining. Recombinant group M consensus gp140 protein was produced and conjugated to Brilliant Violet 421 and Alexa Fluor 647 fluorophores, as previously described (49, 79). Washed PBMCs were pretreated with anti-CD4 (clone SK3, Biolegend) previous to Aqua amine-reactive dye staining to prevent interactions between gp140 probe and CD4. gp140 probe was then added to the surface marker cocktail and staining procedure was completed as described above.

Serum antibody characterization. HIV-1–specific and total IgG1, IgG4, IgA, and IgM were measured on a Bio-Plex instrument (Bio-Rad) as previously described (80–82). gp140-specific antibodies were captured using the same group M consensus sequence protein from gp140-specific cell staining (see above).

Cell sorting and Fluidigm Biomark transcript analysis. PBMCs from HIV-infected and -uninfected patients were thawed and rested overnight. After being washed in PBS, the cells were incubated with Aqua amine-reactive viability dye for 10 minutes and stained with an undiluted cocktail of surface antibodies at room temperature. Cells were washed and resuspended in R10. One hundred cells each from different B cell populations were sorted on a FACSAria II (BD Biosciences) into individual wells of a 96-well PCR plate according to the gating strategy depicted in Supplemental Figure 1A. Each well contained 5 μl lysing buffer, consisting of 4.725 μl of DNA Suspension Buffer (10 mM Tris, pH 8.0, 0.1 mM EDTA; TEKnova), 0.025 μl of 20 U/μl SUPERase•In (Ambion), and 0.25 μl of 10% NP40 (Thermo Fisher Scientific). After FACS sorting, PCR plates were frozen and kept at –80°C until usage.

PCR plates were thawed on ice and preheated for 90 seconds at 65°C. Subsequently, 1 μl Reverse Transcription Master Mix (Fluidigm) was added to each well and placed into a thermocycler for reverse transcription (25°C for 5 minutes, 42°C for 30 minutes, 85°C for 5 minutes). Next, 4 μl of a preamplification mix, consisting of 1 μl pooled mixture of all primer assays (500 nM), 2 μl 5× PreAmp Master Mix (Fluidigm) and 1 μl H_2O, was added to each well and run on a thermocycler (95°C for 5 minutes followed by 18 cycles: 96°C for 5 seconds, 60°C for 6 minutes). To remove excess primers, 4 μl of an exonuclease mixture, containing 0.8 μl 20 units/μl of Exonuclease I (New England BioLabs), 0.4 μl 10× Exonuclease I Reaction Buffer (New England BioLabs), and 2.8 μl H_2O was added to each well. The plate was run on a thermocycler (37°C for 30 minutes, 80°C for 15 minutes). Each well was then diluted (1:4) with DNA

Suspension Buffer. In a new PCR plate, distinct primer assays were generated by adding individual primer pairs (5 μM) together with a mix of 2.6 μl 2× Assay Loading Reagent (Fluidigm) and 2.4 μl 1× DNA Suspension Buffer to each well. Similarly, a sample PCR plate was created by dispensing 4 μl of a sample master mix containing 3.5 μl 2× Sso Fast EvaGreen Supermix with Low ROX (Bio-Rad), 0.35 μl 20× DNA Binding Dye Sample Loading Reagent (Fluidigm), and 0.15 μl H_2O to each well. An additional 3 μl of preamplified samples were added to each well. Control line fluid (Fluidigm) was injected to the 96.96 Dynamic Array chip (Fluidigm) and the chip was primed using an IFX Controller HX. After priming the chip, 4.5 μl of the primer assays and 5 μl of the sample mix were added to detector inlets of the chip and transferred to the IFX Controller HX for loading the mixtures. The chip was then transferred to a Biomark HD instrument (Fluidigm) and run using the GE Fast 96x96 PCR+Melt v2.pcl program. All primers were purchased from IDT and assay efficiency as well as melting and amplification curves for each assay were evaluated beforehand on a separate Biomark HD run with similar sorted B cell populations.

All data were preanalyzed with the Real-Time PCR Analysis software (Fluidigm), and linear (derivative) and user (detectors) were used as settings to generate Ct values. A conservative Ct value of 25 was used as limit of detection (LOD). Relative gene expression was defined as a $\log_2$ value based on: $\log_2$ = LOD – Ct. All subsequent analysis of the gene expression data, including tSNE analysis and hierarchical clustering, were performed using R Studio.

T-bet siRNA knockdown. Mature $CD21^-CD27^-$ B cells from viremic HIV^+ donors were transfected with 500 nM of control nontargeting or *TBX21*-specific ON-TARGETplus SMARTpool siRNAs (Thermo Fisher Scientific) using the Lonza nucleofection 96-well plate system, according to the manufacturer's specifications and as previously described (42). Cells were rapidly transferred to preheated complete medium (RPMI 1640/10% FBS) and incubated for 24 hours at 37°C. Cell viability was evaluated by vital dye exclusion (Guava Technologies). *TBX21* knockdown efficiency and impact on *AICDA* expression were evaluated by quantitative RT-PCR, as previously described (42). Briefly, total RNA was extracted using the RNeasy Micro Kit with on-column DNA digestion (Qiagen), according to the manufacturer's specifications. Total RNA was reverse transcribed and analyzed using TaqMan probe/primer mix (Applied Biosystems) by one-step quantitative PCR (Applied Biosystems 7500 system). Data were normalized to the housekeeping gene *POLRIIA* by a comparative ΔΔCt method.

Statistics. Paired or unpaired t-tests (2-tailed) were used to compare 2 groups of data. When 3 or more groups were compared, 1-way ANOVA or repeated-measures 1-way ANOVA, each combined with Tukey's multiple comparisons test, were used. Correlative relationships were assessed using Spearman correlation. Error bars on all plots represent mean ± SEM. A *P* value less than 0.05 was considered significant.

Study approval. Written informed consent was obtained from study participants and blood samples were collected with IRB approval at each collecting institution: Oregon Health and Science University (IRB 2470, IRB 2832), University of Pennsylvania (IRB 809316, IRB 815056), Case Western University (IRB 10-09-12), University of Toronto (REB 12-378), University of California San Francisco (IRB 10-01330), Human Subjects Protection Branch (RV217/WRAIR 1373), The United Republic of Tanzania Ministry of Health and Social Welfare (MRH/R.10/18/VOLL.VI/85), Tanzanian National Institute for Medical Research (NIMR/HQ/R.8aVol.1/2013), Royal Thai Army Medical Department (IRBRTA 1810/2558), Uganda National Council for Science and Technology–National HIV/AIDS Research Committee (ARC 084), and Uganda National Council of Science and Technology (HS 688). This study was conducted in accordance with the principles expressed in the Declaration of Helsinki.

Author contributions

JJK designed, performed, analyzed, and interpreted experiments and wrote the manuscript. MB helped perform and analyze experiments and offered helpful discussion. LK and KES performed and analyzed additional experiments. MAE, DHC, MLR, MAO, SGD, and MKS supplied critical samples. GDT, SM, and MAM contributed to experimental design and data interpretation and offered helpful discussion. MRB contributed to experimental design, analysis, and interpretation and helped write the manuscript.

Acknowledgments

We would like to thank Lawrence C. Armand for production of the gp140-specific probes, Max C. Cooper for providing clone 2A6 antibody (anti-FcRL4/5), Shad Mosher and Judith Lucas for assistance with serum Ig isotype analyses, and E. John Wherry and Michael P. Cancro for productive discussions. The views

expressed are those of the authors and should not be construed to represent the positions of the US Army or the Department of Defense. This work was supported by a cooperative agreement (W81XWH-11-2-0174) between the Henry M. Jackson Foundation for the Advancement of Military Medicine, Inc., and the US Department of Defense (DOD). Funding sources for this work include NIAID R01 AI076066 (MRB) and T32 AI007632 (JJK). The authors declare no competing financial interests.

Address correspondence to: Michael R. Betts, Department of Microbiology, Perelman School of Medicine, University of Pennsylvania, Philadelphia, Pennsylvania, USA. E-mail: betts@upenn.edu.

1. Global AIDS Update 2016. UNAIDS. http://www.unaids.org/en/resources/documents/2016/Global-AIDS-update-2016. Published May 31, 2016. Accessed March 22, 2017.
2. Fauci AS, Folkers GK, Marston HD. Ending the global HIV/AIDS pandemic: the critical role of an HIV vaccine. *Clin Infect Dis*. 2014;59 Suppl 2:S80–S84.
3. Haynes BF. New approaches to HIV vaccine development. *Curr Opin Immunol*. 2015;35:39–47.
4. Wibmer CK, Moore PL, Morris L. HIV broadly neutralizing antibody targets. *Curr Opin HIV AIDS*. 2015;10(3):135–143.
5. Dörner T, Radbruch A. Antibodies and B cell memory in viral immunity. *Immunity*. 2007;27(3):384–392.
6. Barnett BE, et al. Cutting Edge: B cell-intrinsic T-bet expression is required to control chronic viral infection. *J Immunol*. 2016;197(4):1017–1022.
7. Plotkin SA. Complex correlates of protection after vaccination. *Clin Infect Dis*. 2013;56(10):1458–1465.
8. Tarlinton D, Good-Jacobson K. Diversity among memory B cells: origin, consequences, and utility. *Science*. 2013;341(6151):1205–1211.
9. Barnett LG, et al. B cell antigen presentation in the initiation of follicular helper T cell and germinal center differentiation. *J Immunol*. 2014;192(8):3607–3617.
10. Shen P, Fillatreau S. Antibody-independent functions of B cells: a focus on cytokines. *Nat Rev Immunol*. 2015;15(7):441–451.
11. Vidarsson G, Dekkers G, Rispens T. IgG subclasses and allotypes: from structure to effector functions. *Front Immunol*. 2014;5:520.
12. Seifert M, Küppers R. Human memory B cells. *Leukemia*. 2016;30(12):2283–2292.
13. Kardava L, et al. Abnormal B cell memory subsets dominate HIV-specific responses in infected individuals. *J Clin Invest*. 2014;124(7):3252–3262.
14. Ellebedy AH, et al. Defining antigen-specific plasmablast and memory B cell subsets in human blood after viral infection or vaccination. *Nat Immunol*. 2016;17(10):1226–1234.
15. Liu N, Ohnishi N, Ni L, Akira S, Bacon KB. CpG directly induces T-bet expression and inhibits IgG1 and IgE switching in B cells. *Nat Immunol*. 2003;4(7):687–693.
16. Calame K. Transcription factors that regulate memory in humoral responses. *Immunol Rev*. 2006;211:269–279.
17. Browne EP. Regulation of B-cell responses by Toll-like receptors. *Immunology*. 2012;136(4):370–379.
18. Wang NS, McHeyzer-Williams LJ, Okitsu SL, Burris TP, Reiner SL, McHeyzer-Williams MG. Divergent transcriptional programming of class-specific B cell memory by T-bet and RORα. *Nat Immunol*. 2012;13(6):604–611.
19. Rubtsova K, Rubtsov AV, van Dyk LF, Kappler JW, Marrack P. T-box transcription factor T-bet, a key player in a unique type of B-cell activation essential for effective viral clearance. *Proc Natl Acad Sci USA*. 2013;110(34):E3216–E3224.
20. Szabo SJ, Kim ST, Costa GL, Zhang X, Fathman CG, Glimcher LH. A novel transcription factor, T-bet, directs Th1 lineage commitment. *Cell*. 2000;100(6):655–669.
21. Harris DP, et al. Reciprocal regulation of polarized cytokine production by effector B and T cells. *Nat Immunol*. 2000;1(6):475–482.
22. Peng SL, Szabo SJ, Glimcher LH. T-bet regulates IgG class switching and pathogenic autoantibody production. *Proc Natl Acad Sci USA*. 2002;99(8):5545–5550.
23. Gerth AJ, Lin L, Peng SL. T-bet regulates T-independent IgG2a class switching. *Int Immunol*. 2003;15(8):937–944.
24. Harris DP, Goodrich S, Gerth AJ, Peng SL, Lund FE. Regulation of IFN-gamma production by B effector 1 cells: essential roles for T-bet and the IFN-gamma receptor. *J Immunol*. 2005;174(11):6781–6790.
25. Serre K, et al. CD8 T cells induce T-bet-dependent migration toward CXCR3 ligands by differentiated B cells produced during responses to alum-protein vaccines. *Blood*. 2012;120(23):4552–4559.
26. Knox JJ, Cosma GL, Betts MR, McLane LM. Characterization of T-bet and eomes in peripheral human immune cells. *Front Immunol*. 2014;5:217.
27. Frisullo G, et al. Increased expression of T-bet in circulating B cells from a patient with multiple sclerosis and celiac disease. *Hum Immunol*. 2008;69(12):837–839.
28. Isnardi I, et al. Complement receptor 2/CD21$^-$ human naive B cells contain mostly autoreactive unresponsive clones. *Blood*. 2010;115(24):5026–5036.
29. Becker AM, et al. SLE peripheral blood B cell, T cell and myeloid cell transcriptomes display unique profiles and each subset contributes to the interferon signature. *PLoS One*. 2013;8(6):e67003.
30. Chang LY, Li Y, Kaplan DE. Hepatitis C viraemia reversibly maintains subset of antigen-specific T-bet$^+$ tissue-like memory B cells [published online ahead of print December 7, 2016]. *J Viral Hepat*. https://doi.org/ 10.1111/jvh.12659.
31. Sullivan RT, et al. FCRL5 delineates functionally impaired memory B cells associated with Plasmodium falciparum exposure. *PLoS Pathog*. 2015;11(5):e1004894.
32. Tomaras GD, Haynes BF. HIV-1-specific antibody responses during acute and chronic HIV-1 infection. *Curr Opin HIV AIDS*. 2009;4(5):373–379.

33. Moir S, Fauci AS. Insights into B cells and HIV-specific B-cell responses in HIV-infected individuals. *Immunol Rev*. 2013;254(1):207–224.
34. Moir S, et al. Decreased survival of B cells of HIV-viremic patients mediated by altered expression of receptors of the TNF superfamily. *J Exp Med*. 2004;200(5):587–599.
35. Moir S, et al. Evidence for HIV-associated B cell exhaustion in a dysfunctional memory B cell compartment in HIV-infected viremic individuals. *J Exp Med*. 2008;205(8):1797–1805.
36. Poland JD, Calisher CH, Monath TP, Downs WG, Murphy K. Persistence of neutralizing antibody 30-35 years after immunization with 17D yellow fever vaccine. *Bull World Health Organ*. 1981;59(6):895–900.
37. Hammarlund E, et al. Duration of antiviral immunity after smallpox vaccination. *Nat Med*. 2003;9(9):1131–1137.
38. Edghill-Smith Y, et al. Smallpox vaccine-induced antibodies are necessary and sufficient for protection against monkeypox virus. *Nat Med*. 2005;11(7):740–747.
39. Robb ML, et al. Prospective study of acute HIV-1 infection in adults in East Africa and Thailand. *N Engl J Med*. 2016;374(22):2120–2130.
40. Li H, Borrego F, Nagata S, Tolnay M. Fc receptor-like 5 expression distinguishes two distinct subsets of human circulating tissue-like memory B Cells. *J Immunol*. 2016;196(10):4064–4074.
41. Muramatsu M, Kinoshita K, Fagarasan S, Yamada S, Shinkai Y, Honjo T. Class switch recombination and hypermutation require activation-induced cytidine deaminase (AID), a potential RNA editing enzyme. *Cell*. 2000;102(5):553–563.
42. Kardava L, et al. Attenuation of HIV-associated human B cell exhaustion by siRNA downregulation of inhibitory receptors. *J Clin Invest*. 2011;121(7):2614–2624.
43. Klasse J, Blomberg J. Patterns of antibodies to human immunodeficiency virus proteins in different subclasses of IgG. *J Infect Dis*. 1987;156(6):1026–1030.
44. Mergener K, Enzensberger W, Rübsamen-Waigmann H, von Briesen H, Doerr HW. Immunoglobulin class- and subclass-specific HIV antibody detection in serum and CSF specimens by ELISA and Western blot. *Infection*. 1987;15(5):317–322.
45. Khalife J, et al. Isotypic restriction of the antibody response to human immunodeficiency virus. *AIDS Res Hum Retroviruses*. 1988;4(1):3–9.
46. Ljunggren K, Broliden PA, Morfeldt-Månson L, Jondal M, Wahren B. IgG subclass response to HIV in relation to antibody-dependent cellular cytotoxicity at different clinical stages. *Clin Exp Immunol*. 1988;73(3):343–347.
47. Binley JM, et al. Profiling the specificity of neutralizing antibodies in a large panel of plasmas from patients chronically infected with human immunodeficiency virus type 1 subtypes B and C. *J Virol*. 2008;82(23):11651–11668.
48. Banerjee K, et al. IgG subclass profiles in infected HIV type 1 controllers and chronic progressors and in uninfected recipients of Env vaccines. *AIDS Res Hum Retroviruses*. 2010;26(4):445–458.
49. Moody MA, et al. HIV-1 gp120 vaccine induces affinity maturation in both new and persistent antibody clonal lineages. *J Virol*. 2012;86(14):7496–7507.
50. Lazarevic V, Glimcher LH, Lord GM. T-bet: a bridge between innate and adaptive immunity. *Nat Rev Immunol*. 2013;13(11):777–789.
51. Horns F, et al. Lineage tracing of human B cells reveals the in vivo landscape of human antibody class switching. *Elife*. 2016;5.
52. Arnold JN, Wormald MR, Sim RB, Rudd PM, Dwek RA. The impact of glycosylation on the biological function and structure of human immunoglobulins. *Annu Rev Immunol*. 2007;25:21–50.
53. Stavnezer J. Complex regulation and function of activation-induced cytidine deaminase. *Trends Immunol*. 2011;32(5):194–201.
54. Russell Knode LM, et al. Age-associated B cells express a diverse repertoire of VH and Vκ genes with somatic hypermutation. *J Immunol*. 2017;198(5):1921–1927.
55. Meffre E, et al. Maturational characteristics of HIV-specific antibodies in viremic individuals. *JCI Insight*. 2016;1(3):e84610.
56. Muellenbeck MF, et al. Atypical and classical memory B cells produce Plasmodium falciparum neutralizing antibodies. *J Exp Med*. 2013;210(2):389–399.
57. Rubtsov AV, Rubtsova K, Kappler JW, Jacobelli J, Friedman RS, Marrack P. CD11c-expressing B cells are located at the T cell/B cell border in spleen and are potent APCs. *J Immunol*. 2015;195(1):71–79.
58. Rubtsov AV, et al. Toll-like receptor 7 (TLR7)-driven accumulation of a novel CD11c+ B-cell population is important for the development of autoimmunity. *Blood*. 2011;118(5):1305–1315.
59. Hao Y, O'Neill P, Naradikian MS, Scholz JL, Cancro MP. A B-cell subset uniquely responsive to innate stimuli accumulates in aged mice. *Blood*. 2011;118(5):1294–1304.
60. Moir S, et al. HIV-1 induces phenotypic and functional perturbations of B cells in chronically infected individuals. *Proc Natl Acad Sci USA*. 2001;98(18):10362–10367.
61. Weiss GE, et al. Atypical memory B cells are greatly expanded in individuals living in a malaria-endemic area. *J Immunol*. 2009;183(3):2176–2182.
62. Doi H, Tanoue S, Kaplan DE. Peripheral $CD27^{-}CD21^{-}$ B-cells represent an exhausted lymphocyte population in hepatitis C cirrhosis. *Clin Immunol*. 2014;150(2):184–191.
63. Oliviero B, et al. Skewed B cells in chronic hepatitis C virus infection maintain their ability to respond to virus-induced activation. *J Viral Hepat*. 2015;22(4):391–398.
64. Charles ED, et al. Clonal B cells in patients with hepatitis C virus-associated mixed cryoglobulinemia contain an expanded anergic CD21low B-cell subset. *Blood*. 2011;117(20):5425–5437.
65. Visentini M, et al. Clonal B cells of HCV-associated mixed cryoglobulinemia patients contain exhausted marginal zone-like and CD21 low cells overexpressing Stra13. *Eur J Immunol*. 2012;42(6):1468–1476.
66. Visentini M, et al. Hepatitis B virus causes mixed cryoglobulinaemia by driving clonal expansion of innate B-cells producing a VH1-69-encoded antibody. *Clin Exp Rheumatol*. 2016;34(3 Suppl 97):S28–S32.
67. Weiss GE, et al. A positive correlation between atypical memory B cells and Plasmodium falciparum transmission intensity in cross-sectional studies in Peru and Mali. *PLoS One*. 2011;6(1):e15983.
68. Visentini M, et al. Persistence of a large population of exhausted monoclonal B cells in mixed cryoglobuliemia after the eradication of hepatitis C virus infection. *J Clin Immunol*. 2012;32(4):729–735.

69. Ayieko C, et al. Changes in B cell populations and merozoite surface protein-1-specific memory B cell responses after prolonged absence of detectable P. falciparum infection. *PLoS ONE*. 2013;8(6):e67230.
70. Kövesdi D, Angyal A, Huber K, Szili D, Sármay G. T-bet is a new synergistic meeting point for the BCR and TLR9 signaling cascades. *Eur J Immunol*. 2014;44(3):887–893.
71. Naradikian MS, et al. Cutting edge: IL-4, IL-21, and IFN-γ interact to govern T-bet and CD11c expression in TLR-activated B cells. *J Immunol*. 2016;197(4):1023–1028.
72. Wei C, et al. A new population of cells lacking expression of CD27 represents a notable component of the B cell memory compartment in systemic lupus erythematosus. *J Immunol*. 2007;178(10):6624–6633.
73. Saadoun D, et al. Expansion of autoreactive unresponsive $CD21^{-/low}$ B cells in Sjögren's syndrome-associated lymphoproliferation. *Arthritis Rheum*. 2013;65(4):1085–1096.
74. Schmitz JE, et al. Effect of humoral immune responses on controlling viremia during primary infection of rhesus monkeys with simian immunodeficiency virus. *J Virol*. 2003;77(3):2165–2173.
75. Deeks SG, et al. Neutralizing antibody responses against autologous and heterologous viruses in acute versus chronic human immunodeficiency virus (HIV) infection: evidence for a constraint on the ability of HIV to completely evade neutralizing antibody responses. *J Virol*. 2006;80(12):6155–6164.
76. Miller CJ, et al. Antiviral antibodies are necessary for control of simian immunodeficiency virus replication. *J Virol*. 2007;81(10):5024–5035.
77. Gaufin T, et al. Limited ability of humoral immune responses in control of viremia during infection with SIVsmmD215 strain. *Blood*. 2009;113(18):4250–4261.
78. Huang KH, et al. B-cell depletion reveals a role for antibodies in the control of chronic HIV-1 infection. *Nat Commun*. 2010;1:102.
79. Williams WB, et al. HIV-1 VACCINES. Diversion of HIV-1 vaccine-induced immunity by gp41-microbiota cross-reactive antibodies. *Science*. 2015;349(6249):aab1253.
80. Tomaras GD, et al. Initial B-cell responses to transmitted human immunodeficiency virus type 1: virion-binding immunoglobulin M (IgM) and IgG antibodies followed by plasma anti-gp41 antibodies with ineffective control of initial viremia. *J Virol*. 2008;82(24):12449–12463.
81. Yates NL, et al. Multiple HIV-1-specific IgG3 responses decline during acute HIV-1: implications for detection of incident HIV infection. *AIDS*. 2011;25(17):2089–2097.
82. Yates NL, et al. Vaccine-induced Env V1-V2 IgG3 correlates with lower HIV-1 infection risk and declines soon after vaccination. *Sci Transl Med*. 2014;6(228):228ra39.